Dynamic analysis of larval locomotion in *Drosophila* chordotonal organ mutants

Jason C. Caldwell, Matthew M. Miller, Susan Wing, David R. Soll, and Daniel F. Eberl*

Department of Biological Sciences, University of Iowa, Iowa City, IA 52242

Edited by Lily Y. Jan, University of California School of Medicine, San Francisco, CA, and approved October 9, 2003 (received for review August 28, 2003)

Rhythmic movements, such as peristaltic contraction, are initiated by output from central pattern generator (CPG) networks in the CNS. These oscillatory networks elicit locomotion in the absence of external sensory or descending inputs, but CPG circuits produce more directed and behaviorally relevant movement via peripheral nervous system (PNS) input. *Drosophila melanogaster* larval locomotion results from patterned muscle contractions moving stereotypically along the body segments, but without PNS feedback, contraction of body segments is uncoordinated. We have dissected the role of a subset of mechanosensory neurons in the larval PNS, the chordotonal organs (chos), in providing sensory feedback to the locomotor CPG circuit with DIAS (Dynamic Image Analysis System) software. We analyzed mutants carrying cho mutations including *atonal*, a cho proneural gene, *beethoven*, a cho cilia class mutant, *smetana* and *touch-insensitive larva B*, two axonemal mutants, and *5D10*, a weak cho mutant. All cho mutants have defects in gross path morphology compared to controls. These mutants exhibit increased frequency and duration of turning (decision-making) and reduced duration of linear locomotion. Furthermore, cho mutants affect locomotor parameters, including reduced average speed, direction change, and persistence. DIAS analysis of peristaltic waves indicates that mutants exhibit reduced average speed, positive flow and negative flow, and increased stride period. Thus, cho sensilla are major proprioceptive components that underlie touch sensitivity, locomotion, and peristaltic contraction by providing sensory feedback to the locomotor CPG circuit in larvae.

Rhythmic movements, such as peristaltic contraction, are initiated by output from central pattern generators (CPGs) in the CNS. These oscillatory networks elicit locomotion in the absence of external sensory or descending inputs, but without feedback from the peripheral nervous system (PNS), contraction of body segments is uncoordinated (1–5). The *Drosophila* peristaltic CPGs form and become active during late embryogenesis and persist throughout larval stages (5–9). Coordinated peristalsis in *Drosophila* embryos, therefore, relies on output from the preformed CPG circuits as well as sensory feedback from the PNS. Here, we use DIAS (Dynamic Image Analysis System) software (10, 11) to demonstrate that chordotonal organs (chos), type I sense organs of the larval PNS (12, 13), constitute a major feedback mechanism that provides peripheral input to the CPG for normal locomotion.

Suster and Bate (5) demonstrated that blocking neurotransmitter release in the entire embryonic PNS with tetanus toxin (TeTx) prevented normal peristalsis during late embryogenesis (14, 15). Interestingly, the peristaltic defects seen in TeTx embryos phenocopied those exhibited in *senseless* (*sens*) null mutants (5, 16). DIAS motility software was used to dissect the dysfunctional locomotor parameters of first-instar TeTx and *sens* larvae and the role of sensory input from the PNS in driving CPGs (5). Wang *et al.* (7, 8) used DIAS to quantify crawling defects in numerous Na^+ and K^+ channel mutants. They found defects both in peristalsis and wandering behavior attributable to motor defects at the neuromuscular junction (NMJ) in third-instar larvae. Barclay *et al.* (17) electrophysiologically recorded synaptic burst activity at the NMJ in *cysteine string protein* (*csp*) mutant larvae, which exhibited synchronous activity bursts at the NMJ but were defective for phase coordination and CNS output generation. These observations suggest that *csp* peristalsis is disrupted at the level of CNS integration. Recently, through targeted expression of TeTx, numerous central neurons that contribute to the larval locomotor CPG were identified, and their characterization is underway (18). Together, these data support the idea that many levels of integration at the PNS, NMJ, and CNS are necessary to produce rhythmic patterns of movement via the CPG circuit.

Using DIAS analysis of mutants (Table 1), we show that chos are a major proprioceptive component that underlies normal locomotion and peristaltic contraction by providing sensory feedback to the locomotor CPG circuit in *Drosophila* larvae.

Materials and Methods

Animals. Genetic strains of *Drosophila melanogaster* included eight mutant strains and two normal controls. *beethoven* (*btv*) larvae from the homozygous *w; btv^{5P1} P{FRT, neo}40A P{FRT, w^{+mC}}G13* strain (19) will be referred to as btv^1 in this paper. The btv^2 larvae were derived from a stock maintained for 2 years as *w; P{lacW, w^{+mC}}k07109a P{lacW, w^{+mC}}k07109b/Df(2L)cact255^{rv64}*. The *5D10* mutant larvae were from a homozygous *w; P{FRT, neo}40A P{FRT, w^{+mC}}G13 5D10* strain. Mutant *touch-insensitive larva B* (*tilB*) larvae [$tilB^1$ or $tilB^2$ alleles (20)] were selected based on *y* mouth parts from stocks in the form *y w tilB/FM4*. Mutant *smetana* (*smet*) larvae were selected by *y* mouth parts among the progeny of crosses between *y w; nompC^1 smet cn bw/CyO, y^+* and *y w; Df(2L)Rev18/CyO, y^+* strains. Larvae mutant for *atonal* (*ato*) (21) were collected from a stock maintained for 6 years as ato^1/$Df(3R)p^{13}$. The *w; norpA^{p12}* strain (22) was used as a negative control for the Darth Vader phototaxis assay. The two control strains were the *w; P{FRT, neo}40A P{FRT, w^{+mC}}G13* strain, which we call *40AG13* in this paper and which carries the genetic background chromosome for the btv^1 and *5D10* mutations (19), and the *y w* strain, which carries the genetic background chromosome for the two *tilB* mutations. Larvae used in all behavior assays were derived from 10-h egg collections (yeasted apple juice agar plates containing 0.5% charcoal for contrast), subsequently aged for 80 h at 25°C and 70% humidity under a 12-h light/12-h dark cycle. These are early third-instar larvae at the foraging stage; thus, we refer to them as "foraging" larvae to distinguish them from the later "wandering" stage. Behavior experiments were conducted within 6 h after lights on.

Agar Substrates and Handling. Assays were performed on 1% agarose in distilled water on Petri dishes. Several sizes were used: 60 mm round (Falcon) with 5 ml of agarose for peristalsis recording, 100 mm round (Falcon) with 15 ml of agarose for locomotor path analysis and for the touch sensitivity assay, and 100 mm square (Lab-Tek) with 15 ml of agarose for the Darth Vader assay. Individual larvae were selected and washed briefly with distilled water to remove any remaining food, transferred with a soft paintbrush to the center of a fresh experimental plate,

This paper was submitted directly (Track II) to the PNAS office.

Abbreviations: cho, chordotonal organ; CPG, central pattern generator; PNS, peripheral nervous system.

*To whom correspondence should be addressed at: Department of Biological Sciences, University of Iowa, Iowa City, IA 52242-1324. E-mail: daniel-eberl@uiowa.edu.

Table 1. Summary of cho mutants used

Gene	Symbol	cho class	Ref.
atonal	*ato*	Specification	21, 25, 37
beethoven	*btv*	Ciliary	19, 25
touch-insensitive larva B	*tilB*	Axonemal	20, 25
smetana	*smet*	Axonemal	38
5D10	*5D10*	Courtship defective	19, 38

ato encodes a proneural bHLH protein that specifies cho precursor cells. In *ato* mutants, chos are absent in both adults and larvae. *btv* is a cho mutant that exhibits ultrastructural defects in the cho cilium, whereas *smet* and *tilB* mutants show male sterility in addition to deafness, suggesting specific defects of the axoneme. Finally, *5D10* mutants, found in a courtship defective auditory behavioral screen, show moderate cho dysfunction.

and allowed between 30 and 60 s to recover from handling. For video recordings and touch analysis, plates were situated over a dark field and illuminated from above with a fiber optic light source to maximize contrast for DIAS analysis.

Touch Sensitivity Assay. Touch sensitivity was tested on single larvae during bouts of linear locomotion at 25°C as in ref. 20, with minor modifications. A score of 0 was given to those larvae that did not respond to gentle touch with an eyelash on their thoracic segments. Larvae that stopped or hesitated were scored as 1, those that retracted briefly but continued their forward locomotion were scored as 2, those that retracted and turned away from the stimulus <90° were scored as 3, and those that retracted and turned away from the stimulus >90° were given a score of 4. Each larva was gently touched and scored four times during linear locomotion. These values were summed to yield a range of possible scores from 0 to 16.

Embryo Staining Methods. Embryos were washed with distilled water, dechorionated 5 min with 50% bleach, and rinsed, then permeabilized and fixed in equal parts of heptane and 4% paraformaldehyde in PBS with gentle agitation for 20 min. Embryos were devitellinized by removing the aqueous phase and most of the heptane phase, then adding absolute methanol and shaking vigorously for 1 min. The supernatant was removed and the devitellinized embryos in the methanol were washed three times in fresh methanol. For labeling, embryos were rehydrated in a methanol series in PBS (70%, 50%, and 30% for 5 min each with gentle agitation) with a final 15 min wash in PBS. After two further 15-min washes in PBT (PBS with 0.5% BSA and 0.2% Triton X-100) for blocking, the embryos were incubated with the primary antibody (rabbit α-HRP antiserum, Cappel; 1:200) in PBT overnight at 4°C with gentle agitation. Primary antibody was removed with four washes in PBT for 30 min each at room temperature. Embryos were then incubated in secondary antibody (TRITC-conjugated goat α-rabbit-IgG antiserum, Sigma; 1:500) in PBT for 2 h at room temperature with agitation. After four washes in PBT for 20 min each, embryos were mounted in VectaShield (Vector Laboratories) and examined with an Olympus BX51 (Melville, NY) compound fluorescence microscope with a ×100-objective lens to score for defects in lateral chos. Images for publication were obtained with a Zeiss confocal microscope.

Video Recording of Locomotor Behaviors. Video recordings of gross path morphology were made with a digital video (DV) camera (Canon GL1) in an environment room maintained at 25°C and 70% humidity. DV movies were captured with IMOVIE 2.0 on a 500-MHz Apple iMac and digitized with QUICKTIME 4.0 at 29.97 frames per second (fps). Low-magnification videos were recorded for 2 min or until the larva left the 50-cm^2 field of the camera. High-magnification videos (15-cm^2 field) were recorded with an Olympus OLY-200 camera mounted on an Olympus SZX9 microscope connected to a VCR (Samsung VR5599). Peristalsis was recorded until 10 peristaltic waves during linear locomotion were completed. Mutants frequently had discontinuous bouts of peristalsis, and repositioning of the plate was necessary, but this did not affect the motion analysis. VCR recordings were captured with ADOBE PREMIER 5.0 on a Macintosh G4 at 15 fps.

DIAS Analysis. DIAS 3.7 was used for all locomotor analysis. Larval perimeters were automatically traced from the high-contrast digital movie frames with the "autotrace by threshold" function. Centroid positions were determined in each traced frame from the x, y coordinates of the pixels constituting each larval outline, generating a path of interconnected centroids (10). "Centroid paths" were generated by plotting each centroid of a traced video segment in its relative x, y position. "Perimeter stacks" were generated by displaying the traced larval perimeters in overlapping series in their relative x, y positions.

"Speed," "Direction Change," "Persistence," "Maximum Length," "Positive Flow," and "Negative Flow" parameters were all calculated automatically in DIAS as described (10, 11). "Stride Period" was determined from a plot of body length vs. time, which was smoothed two to three times with a Tukey window of 5, 15, 60, 15, 5. Peaks of peristaltic waves were determined by using the "find maxima" function of DIAS.

Turns and retreats were analyzed manually. Turns are defined as changes in direction that were <30° followed by linear locomotion. Retreats are direction changes >30° followed by linear locomotion.

All locomotion data were statistically tested for effects of differences in larval size by using the "Area" function of DIAS; this was found to have no significant effect on the outcomes.

Darth Vader Assay. We used a slightly modified version of the Darth Vader assay (23). We illuminated an agarose plate from beneath with a Fisher white light transilluminator and prevented light from entering one half of the plate with aluminum foil ("the dark side") while the other side was lit. Single larvae were placed on the midline of the test plate and observed for 90 s ($n = 10$) or until the larva contacted the edge of the plate.

Statistical Analysis. All data were analyzed by using SAS 6.12 or JMP 4.0 (SAS Institute, Cary, NC). Touch sensitivity, gross path morphology, and peristaltic wave data were analyzed by the General Linear Method and subsequently by the Dunnett's test with the *40AG13* control as the model. Phototaxis data were analyzed by χ^2.

Results

cho Mutants Are Touch-Insensitive. Peripheral input to the CPG during larval locomotion could occur externally when the larva encounters an object or when an object, such as another larva, bumps into it. Peripheral mechanoreceptors could also be activated by the muscle contractions that mediate locomotion. To distinguish these internal vs. external effects, we tested for external touch sensitivity. Kernan *et al.* (20) developed a reliable technique for assaying touch sensitivity in larvae (see *Materials and Methods*). A gentle eyelash-stroke to the anterior end of a larva during free-run locomotion could stimulate any of the putative PNS mechanosensory components found in each segment, such as chos, campaniform sensillae, multidendritic (md) neurons, and sensory hairs (12, 13, 20). These mechanosensory elements may all have a role in eliciting a response to touch (i.e., locomotion); therefore, our goal was to determine the extent to which touch sensitivity was affected in our array of cho mutants (Table 1).

Control strains (*40AG13* and *y w*) both had a strong response to touch ($\bar{x}$ = 7.05 and 7.7), whereas all cho mutants had diminished sensitivity to touch (Fig. 1). The axonemal class mutants, *smet*, *tilB*^{1}, and *tilB*^{2}, as well as both *btv* alleles and *ato* had almost no response to touch. The mutant that exhibited only

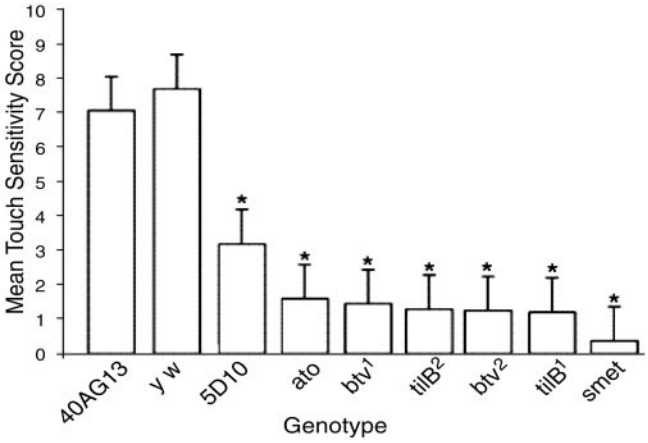

Fig. 1. Touch-insensitivity of cho mutants. Shown is the mean touch sensitivity histogram with standard deviation bars. *, Significant difference from *40AG13* by Dunnett's test ($P < 0.05$). $n = 50$ for all genotypes except *5D10*, where $n = 65$. All cho mutants have strongly reduced touch sensitivity compared to *40AG13*, whereas the additional control, *y w*, has normal touch sensitivity.

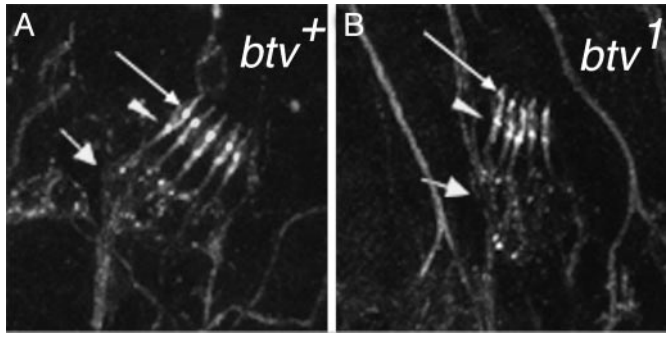

Fig. 2. Morphological defects in cho mutants. Late-stage embryos were stained with α-HRP as detailed in Table 2. Shown are abdominal hemisegments of a control embryo (*40AG13*) (A) and a *btv*^{1} mutant embryo (B). The *btv* mutants showed a high frequency of outer dendritic segment defects, especially the lack of a clear ciliary dilation (thin arrow). The inner dendritic segments, from the soma (thick arrow) to the basal bodies (arrowhead), appeared relatively normal in *btv* mutants compared to the *40AG13* controls. We found no obvious defects in the *5D10* mutants (not shown; see also Table 2), which are the weakest of our cho mutants.

partial dysfunction of chos, *5D10*, had a moderate but still significant ($\bar{x} = 3.18$) reduction in touch sensitivity (Fig. 1).

Morphological Defects in cho Mutants. These results suggest that the touch sensitivity of larvae is mediated primarily by the chos. Each of the mutants has been shown to have normal electrophysiological responses in adult bristle organs. Previously, *ato* mutants had been shown to lack chos and a subset of md neurons in the larval thoracic and abdominal segments (21, 24). In the other cho mutants under study, the chos are present and specified properly; thus, the defects in these mutants may be either morphological defects in the differentiation of the chos or physiological defects that disrupt their function. Ultrastructural analysis of antennal chos in the *btv* mutant adults showed ciliary defects (25), but larval chos were not examined. Ultrastructural defects in sperm tail axonemes in *tilB* mutants (25) suggest that cho defects would be too subtle to detect by light microscopy; indeed, *tilB* mutants had been found to have normal larval cho morphology when stained with mAb 22C10 or mAb 21A6 (20), although these reagents do not stain the ciliated outer dendritic segment very well. Our preliminary results suggest that the *smet* sperm tail phenotype is similar to that of *tilB*; that is, frequent split axonemes (R. G. Kavlie, E. Loukianova, and D.F.E., unpublished observations). Although we were thus unlikely to see morphological defects in *tilB* and *smet*, the fact that *btv* and *5D10* mutants can be maintained as homozygous stocks allowing the collection of large numbers of unmarked embryos led us to examine mutants in these two genes for morphological defects in embryonic chos in a blind experiment. For this experiment, we stained the embryos with α-HRP, which labels all neurons but in chos preferentially labels the dendrites, including the ciliated outer dendritic segment.

The results of this analysis are shown in Table 2. We found significant disruptions of outer dendritic segment morphology in both *btv* alleles, with a very consistent loss of identifiable ciliary dilation. Examples of these defects are shown in Fig. 2. We found neither significant loss of scolopidia nor significant defects in arrangement of the five scolopidia within each lch5 cluster. The *5D10* mutant exhibited no defects that we could detect with this analysis. These results and considerations indicate a morphological basis for cho dysfunction in *btv* and *ato* mutants, whereas in *5D10*, *tilB*, and *smet* mutants, cho dysfunction must be explained either by ultrastructural or purely physiological defects.

Foraging cho Mutant Larvae Exhibit Locomotor Defects in Gross Path Morphology. The observation that *tilB* and *btv* adults have reduced and uncoordinated motility led us to assay the degree to which locomotor defects were exhibited by cho mutant larvae. We used DIAS to quantify the locomotor patterns of control and mutant larvae during stimulus-free conditions.

Foraging larvae have bouts of linear crawling and periods of

Table 2. Morphological defects in cho mutants

	Individual scolopidia				Whole lch5 organs				
Genotype	*n*	% missing scolopidia	% ODS affected	% cd missing	*n*	% plane	% row	% spacing	% orientation
btv^1	1,690	2.5	46.4***	98.7*	338	22.0	3.6	1.2	3.0
40AG13	2,310	1.9	0.7	14.3	462	18.2	5.0	1.0	1.7
btv^2	1,960	0.8	86.6***	98.9**	397	7.8	5.8	1.3	2.3
40AG13	1,870	1.0	0.4	17.0	374	19.0	0.5	1.6	0
5D10	2,180	1.0	0.6	5.0	436	20.4	2.8	2.8	0.2
40AG13	1,690	1.1	0.3	6.8	338	36.1	5.9	5.0	6.8

Embryos stained with α-HRP to label neurons, particularly the ciliary part of the dendrite, were scored blind with respect to the genotype of embryos on each slide. Whole pentascolopidial organs (lch5) in the seven abdominal segments were examined for defects in arrangement of the five units, with scores for plane (ie mediolateral alignment), row (dorsoventral alignment), spacing, and relative orientation. Within the lch5 clusters, individual scolopidia were scored for presence, morphology of the outer dendritic segment (ODS) and visibility of the ciliary dilation (cd). Statistics for each column were tested by Dunnett's test using the pooled *40AG13* data as the control and the relevant *n*s as weighting factors. *, $P < 0.05$; **, $P < 0.01$; ***, $P < 0.001$.

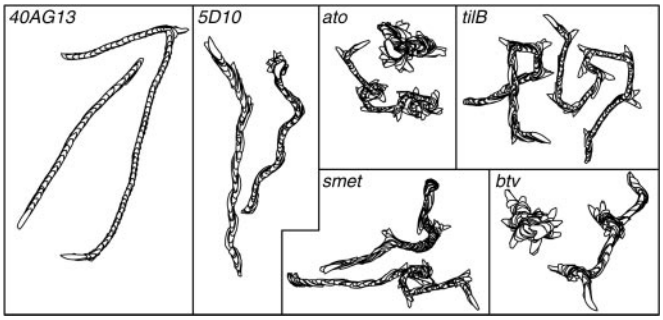

Fig. 3. Representative larval perimeter stacks for gross path morphology video recordings analyzed in DIAS. Controls have directional locomotion with infrequent turns and regular displacement of centroids. cho mutants exhibit gross defects in wandering behavior. These mutants have more frequent decision-making bouts (darker, overlapping perimeter stacks) and reduced centroid displacement. Most noticeably, *ato* and *btv* have ''directionless'' paths much more frequently than the axonemal class mutants (*tilB* and *smet*) and *5D10*. The panels in this figure are set to varying scales to augment the presentation of path defects.

pausing, the so-called decision-making component of locomotion (7). The perimeter stacks of representative larvae from each genotype used in this study illuminate the decision-making behavior (Fig. 3). Cho mutants have frequent periods of pausing that can be visualized in the perimeter stacks as darker, overlapping images strongly evident during periods of decision-making (Fig. 3). Furthermore, the duration of linear locomotion between episodes of pausing and turning was reduced in all cho mutants. Control larvae exhibit more regular and persistent linear locomotion, with fewer and shorter intervals of decision-making and turning. With these observations of dysfunction in overall crawling morphology, we used DIAS to determine the specific nature of the defects affecting locomotion in cho mutants, including (*i*) average speed, (*ii*) direction change, (*iii*) persistence, and (*iv*) total path length, in addition to manual analysis of frequency of retreats and turns (Table 3).

DIAS analysis indicates that cho mutants deviate from controls in average direction change. Similarly, manual analysis of video recordings revealed a significant increase in the frequency of turns or retreats in all mutants, with the exception of *5D10*. Persistence is calculated as the relationship between speed and direction change and is a measure of turning in a moving object. If the object is not turning, speed and persistence produce the same value. Persistence in all cho mutants is strongly reduced compared to controls. Furthermore, all cho mutants showed significant reduction of total path length. *ato* and *btv* exhibited the strongest reduction of total path length, whereas the axonemal mutants and *5D10* were not as strongly affected (Table 3).

We conclude from these data that several aspects of larval locomotion in mutants with cho dysfunction are aberrant. Furthermore, we can separate classes of cho mutants on the basis of their overall path morphology. The most extreme path defects are seen in *btv* and *ato*, whereas moderate defects are seen in *5D10*.

cho Mutants Exhibit Defects in Peristaltic Contraction. To determine whether individual patterns of peristaltic waves are affected in these mutations, we used high-magnification recordings to analyze larval peristalsis during linear locomotion. Using DIAS, we compared maximum and minimum body lengths during single waves of contraction, stride period, average speed, and mean positive and negative flow. Similar to the gross morphological data, mutant larvae frequently changed direction after a few waves of contraction, but this discontinuity of peristalsis did not affect the analysis because frames of decision-making were not traced.

One of the most significant parameters affected by the mutants in the gross morphological analysis is larval speed. We wanted to determine whether defects in individual peristaltic waveforms were the cause of reduced speed in cho mutants. We used the high-magnification recordings to measure mean positive and negative body flow (extension and retraction, respectively) and plot centroid displacement during a single peristaltic contraction. Control larvae exhibit a regular pattern of centroid displacement and stereotypical positive and negative flow during peristalsis (7). In all cho mutants, both centroid displacement over a single peristaltic wave (data not shown) and negative and positive flow were reduced compared to controls (Table 4). Furthermore, the body is often maintained in an extended position in *btv* and *ato* larvae, whereas *smet* and *tilB* generally spend the majority of a single peristaltic cycle in a retracted position. In the axonemal class, the positions of centroids during the contraction cycle were much denser at the beginning of peristaltic wave (trough), often with little movement of the anterior end of the larvae. In *btv* and *ato*, centroids piled up at the peaks of a contraction cycle (data not shown); much of the initial anterior movement occurred in these mutants in the first phase of the peristaltic wave before pausing at the maxima and posterior end retraction. The data in Table 4 correlate well with these observations; average maximum body length is significantly larger in *ato* and *btv* mutants but not in the *5D10*, *smet*, and *tilB*. There was no significant difference in minimum body length in any of the mutants, indicating that the retracted body length is unchanged in defective larvae. However, there are strong reductions in mean positive and negative flow for all cho defective classes.

Table 3. Analysis of gross path morphology data

	40AG13	*y w*	*5D10*	*ato*	*btv*[1]	*btv*[2]	*smet*	*tilB*[1]	*tilB*[2]
n	30	30	36	36	27	31	31	30	30
Avg. speed, cm/s	0.096 ± 0.01	0.102 ± 0.02	0.033 ± .009*	0.033 ± .008*	0.031 ± .0017*	0.029 ± .005*	0.044 ± 0.01*	0.059 ± .009*	0.057 ± 0.011*
Avg. DC, degrees	40.92 ± 6.9	44.67 ± 6.99	54.64 ± 10.3*	54.01 ± 10.0*	57.41 ± 9.89*	58.53 ± 8.26*	71.40 ± 10.2*	57.93 ± 8.92*	67.91 ± 8.73*
Avg. turns	0.83 ± 1.31	1 ± 1.41	0.97 ± 1.13	1.61 ± 1.27	0.85 ± 1.06	0.74 ± 0.77	1.96 ± 2.1*	2.6 ± 1.61*	1.46 ± 1.22
Avg. retreats	0.4 ± 0.96	0.36 ± 1.06	2 ± 1.51	3.55 ± 2.66*	3.51 ± 2.35*	3.90 ± 2.63*	0.81 ± 1	2.16 ± 2.21*	1.76 ± 2.01*
Persistence, grads	0.036 ± .008	0.033 ± .009	0.008 ± .003*	0.008 ± .003*	0.007 ± .003*	0.006 ± .002*	0.008 ± .004*	0.015 ± .005*	0.012 ± .004*
Avg. path, cm	21.07 ± 5.48	20.77 ± 5.02	10.08 ± 6.3*	8.02 ± 5.72*	5.69 ± 5.39*	5.51 ± 6.21*	10.93 ± 8.11*	14.48 ± 5.67*	12.41 ± 6.79*

The parameters of speed and persistence were reduced in all cho mutants as compared to wild type. The cho mutants show increased average direction change (DC) and increased turns and retreats, indicating reduced persistence. cho mutants also had reduced total path length. Data are presented as mean ± SD. *, Significant difference by Dunnett's test compared to *40AG13*, $P < 0.05$.

Table 4. Analysis of peristaltic wave data

Parameter	*40AG13*	*y w*	*5D10*	*ato*	*btv*[1]	*btv*[2]	*smet*	*tilB*[1]	*tilB*[2]
Speed, mm/s	0.922 ± 0.63	0.77 ± 0.6	0.415 ± 0.37*	0.49 ± 0.36*	0.476 ± 0.34*	0.533 ± 0.4*	0.45 ± 0.35*	0.65 ± 0.45*	0.55 ± 0.45*
Maximum length, mm	3.69 ± 0.28	3.93 ± 0.25	4.06 ± 0.51	4.12 ± 0.29*	4.1 ± 0.25*	4.24 ± 0.22*	3.86 ± 0.47	3.82 ± 0.27	3.82 ± 0.46
Minimum length, mm	3.16 ± 0.24	3.47 ± 0.29	3.27 ± 0.41	3.32 ± 0.3	3.09 ± 2.96	3.55 ± 0.22	3.29 ± 0.47	3.27 ± 0.23	3.27 ± 0.44
Mean positive flow, %	3.54 ± 1.66	3.84 ± 1.92	1.87 ± 0.74*	2.33 ± 0.9*	2.87 ± 0.225*	2.78 ± 1.35*	2.09 ± 0.81*	2.79 ± 1.21*	2.79 ± 1.21*
Mean negative flow, %	3.5 ± 1.64	3.8 ± 1.85	1.85 ± 0.81*	2.34 ± 1.02*	2.734 ± 1.58*	2.77 ± 1.44*	2.08 ± 0.87*	1.19 ± 1.19*	2.76 ± 1.19*
Stride period, s	1.05 ± 0.26	1.02 ± 0.21	1.79 ± 0.49*	1.93 ± 0.83*	2.08 ± 0.32*	2.08 ± 0.32*	2.03 ± 0.65*	1.88 ± 0.21*	2.14 ± 0.79*

cho mutants are defective for numerous parameters in each contraction cycle. As in the gross path morphology analysis (Table 3), speed was reduced in all mutants. Maximum body length was significantly higher for both *btv* alleles and for *ato,* whereas the axonemal class cho mutants, *tilB* and *smet,* and the weak mutant, *5D10,* were not different from *40AG13* and *y w* controls. Minimum body length was unaffected in all classes. Positive flow and negative flow were reduced in all cho mutants. Overall, cho mutants have a 2-fold increase in stride period during a single peristaltic contraction. Data are presented as mean ± SD. *, Significant difference by Dunnett's test compared to *40AG13*, $P < 0.05$. $n = 10$ larvae for all genotypes and 10 peristaltic waves were analyzed per larva.

We used perimeter stacks of larvae to elucidate the morphological abnormalities of peristaltic waves that are attributable to the positive and negative flow defects seen in cho mutants (Fig. 4, which is published as supporting information on the PNAS web site, and Table 4). In *40AG13* and *y w* control strains, perimeter stacks appear normal: linear locomotion, with little or no left and right drift, and stereotypic displacement of the body perimeter with brief periods of pause between peristaltic waves, where the stacked images amass, producing a noticeable boundary between contraction cycles. Conversely, perimeter stacks of all cho classes exhibit frequent left and right drift, increased head swings, reduced interperistaltic distance, and increased stacking of perimeter traces during and between each new contraction cycle. All of these data together suggest that cho dysfunction results in defects in individual peristaltic waves that can produce the reduced larval speed and abnormal paths found in the low-magnification DIAS analysis of gross path morphology (Tables 3 and 4 and Figs. 3 and 4).

Change in maximum body length is significantly increased in *ato* and *btv* larvae (Table 4). Unlike *40AG13* and *y w*, *ato* and *btv* larvae tend to remain in an extended position at the apex of a single wave of contraction significantly longer but are largely unaffected during the contracted, trough, phase. Similarly, there are brief plateaus in the peaks of the axonemal class, but average *maximum* body length is not different from controls (Table 4), suggesting that mutants in this class do not tend to remain in an extended position during a contraction cycle. In *tilB* and *smet* mutants, however, the visible defect is in the troughs between contraction cycles. As mentioned above, the axonemal mutants often spend more time in the retracted position and initiate movement from this position by drifting left and right, or by anterior head swings. Overall, cho mutants exhibit a 2-fold longer stride period than controls (Table 4 and Movie 1, which is published as supporting information on the PNAS web site).

cho Mutants Exhibit Normal Phototaxis. To determine whether the motility defects in cho mutants result from loss of sensory feedback rather than defects in core CPG function or motor output, we used a simple photobehavior test, the Darth Vader assay (23). This assay is an excellent measure of phototactic defects because control third-instar foraging larvae show a stereotypic preference for dark areas (26). If movement can be coordinated enough to "go to the dark side," then cho mutants should exhibit a nonrandom preference for the nonilluminated half of the testing arena. Another negative control genotype, *no receptor potential A* (*norpA*), was used. This mutant was previously shown to display no preference for either light or dark conditions (22).

In light/dark choice, cho mutants are able to coordinate movement toward the dark side (Table 5). Similar to defects seen in *norpA*, *ato* and *smet* mutants demonstrated no preference for light or dark. During patterning of the embryonic visual system, *ato* is required for development of Bolwig's Organ, the larval photoreceptive organ (27, 28). The larval phototactic defect can therefore be attributed to loss of *ato* expression in Bolwig's organ founder cells. Adult *smet* flies have normal electroretinogram responses; therefore, the origin of the *smet* larval defects in phototaxis is unclear. Nevertheless, the other cho mutants provide strong support for the conclusion that locomotor defects are explained by loss of cho feedback to the CPG rather than to core CPG function or motor output.

Discussion

Movement is elicited by the CPG in the absence of peripheral input, but sensory feedback provides additional behaviorally relevant information to the organism to produce coordinated and rhythmic motility (5). Our analysis of locomotion in *Drosophila* third-instar foraging larvae demonstrates that chos are major modulators of rhythmic peristalsis. High-magnification recordings of individual waves of contraction indicated that despite the defects in single waves of contraction, cho mutants were able to generate peristaltic waves that showed centroid advancement but lacked coordination of body segments during peristalsis. Our analyses indicate that sensory feedback from the cho pathway onto the CPG is dysfunctional in all of our mutants, leading to aberrant centroid tracks and peristaltic contractions.

Table 5. Phototactic behavior in cho mutants

Genotype	*n*	χ^2 (*P* value)
40AG13	10	0.001
y w	10	0.007
5D10	10	0.007
ato	10	0.074*
btv[1]	10	0.002
btv[2]	10	0.002
tilB[1]	10	0.001
tilB[2]	10	0.002
smet	10	0.655*
norpA	10	0.655*

The cho mutant larvae respond to a simple light stimulus and clearly "go to the dark side" of a testing arena. *ato* and *norpA* mutants served as negative controls for this assay because both strains have previously been shown to have no preference for light or dark. Data are presented as χ^2 probability for no preference on light/dark regimes (50:50). *, No significant difference from neutral preference.

Comparing *sens* and *ato* mutants, a striking parallel between motility defects is found: both mutants produce rhythmic activity and exhibit strong defects in coordination (5). First-instar larvae lacking PNS show disruptions primarily in backward movement at the expense of forward bursts (5). All parameters in our gross path analysis are consistent with more frequent retreats and strong reduction in forward movement in cho mutants. Thus, loss of cho function largely accounts for the locomotor defects seen with loss of the entire PNS. Although *ato* removes chos, it also removes a subset of md neurons (21). However, the *ato*-dependent subset of md neurons appears to contribute very little to the PNS feedback because *ato* resembles the other cho mutants in most parameters of the gross path morphology as well as the peristaltic analysis. Do other putative mechanosensory elements of the PNS contribute feedback to the locomotor CPG? A third-instar larva at the foraging stage moving across the surface of an agarose plate has only minimal opportunity for the external sensory organs to be stimulated, with the exception of the campaniform subclass. If the larvae were allowed to burrow in the medium, sensory hairs would more likely be stimulated. The md neurons independent of *ato* are candidates for feedback, although a mechanoreceptive function has not been shown for md neurons; indeed, many are found to respond to temperature (29), and a subset were recently shown to have nociceptive function (30). It will be important to determine the contribution of these other sensory classes to the locomotor CPG regulation. Nevertheless, the similarity of locomotor defects in our third-instar cho mutants to those of embryos or first-instar larvae lacking PNS function (5) suggests that these other classes may supply relatively minor input to the CPG. Alternatively, other PNS elements may contribute a qualitatively different kind of modulation or regulate the polarity of movement by complementary input.

The causes of cho dysfunction may be different in each mutant. As mentioned above, *ato* lacks larval chos (21), whereas *tilB* and *5D10* (this work) have morphologically normal chos at the level of light microscopy. Both *btv* alleles display clear loss of ciliary dilation structure but otherwise appear intact. The overall similarity in locomotor defects in these cho mutants in diverse classes highlights their effects on common sense organs, the chos.

Moreover, the severity of the locomotor defects correlates, in general, with the severity of cho dysfunction in each mutant. However, there are also some mutant-specific effects on locomotion, touch sensitivity, and phototactic behavior that appear anomalous. A possible explanation for these differences is the fact that the gene products and expression patterns of most of these genes are not yet known and may not be limited to chos. In addition, we have not ruled out for every mutant the possibility of second-site mutations that could modify or independently affect these behaviors, although our use of multiple alleles for *btv* and *tilB*, and our use of a noncomplementing deficiency for *smet*, mitigates this problem. Therefore, the broad agreement in results with different cho mutants strongly supports the conclusion that chos provide major feedback to the locomotor CPG.

The Darth Vader assay demonstrated that most cho mutants are able to direct their movement, albeit in an uncoordinated manner, away from a light stimulus. We believe this strengthens the argument that the locomotor defects detected in the absence of external stimuli are primarily due to dysfunction of peripheral input from the chos on the CPG circuit. This input from the larval chos is analogous to the defect seen in adults, wherein flies are flightless and show a degree of uncoordination and sedentary behavior (in addition to being deaf) due to dysfunction of leg and wing chos.

The reduction of many parameters in gross paths is statistically similar in all cases, but perimeter stack images reveal intriguing differences in paths of the axonemal, nonaxonemal, behavioral, and patterning classes. Similarly, differences in centroid piling during a single wave of peristaltic contraction can discriminate between the axonemal class and *btv*; the peaks/plateaus in *btv* and troughs in axonemal class mutants are aberrant, suggesting that differences in defects in the ultrastructure of a cho will produce different, but predictable, peristaltic defects. This is particularly interesting when considering the number of touch sensitivity and locomotor mutants that have been identified as molecular components of the cho (19, 20, 25, 31–36) and whose defects in larval locomotion are likely to be similar to those presented in this article. A more thorough understanding of the role of these genes in mechanosensation and their effects on feedback to the CPG will be possible through identification and characterization of their gene products.

We thank Wayne Johnson, Grace Boekhoff-Falk, Lyle Fox, and Ana Campos for critical reading of versions of the manuscript, Maurice Kernan, Chun-Fang Wu, Randy Hewes, Andrew Jarman, and the Bloomington *Drosophila* stock center for providing fly stocks, and the University of Iowa W. M. Keck Facility, Developmental Studies Hybridoma Bank, and Central Microscopy Research Facility. D.R.S. was supported by National Institutes of Health Grant HD18577. J.C.C. was supported, in part, by a fellowship from the Developmental Studies Hybridoma Bank at the University of Iowa. S.W. was supported, in part, by a Howard Hughes Undergraduate Summer Research Program Fellowship. D.F.E. was supported by National Institutes of Health Grant DC04848 and a Whitehall Foundation grant.

1. Dickinson, M. H., Farley, C. T., Full, R. J., Koehl, M. A. R., Kram, R. & Lehman, S. (2000) *Science* **288,** 100–106.
2. Pearson, K. G. (1995) *Curr. Opin. Neurobiol.* **5,** 768–791.
3. Marder, E. & Bucher, D. (2001) *Curr. Biol.* **11,** R986–R996.
4. Marder, E. (2002) *Nature* **416,** 131–132.
5. Suster, M. L. & Bate, M. (2002) *Nature* **416,** 174–178.
6. Pereira, H. S., MacDonald, D. E., Hilliker, A. J. & Sokolowski, M. B. (1995) *Genetics* **141,** 263–270.
7. Wang, J. W., Sylwester, A. W., Reed, D., Wu, D.-A. J., Soll, D. R. & Wu, C.-F. (1997) *J. Neurogenet.* **11,** 231–254.
8. Wang, J. W., Soll, D. R. & Wu, C.-F. (2002) *J. Neurogenet.* **16,** 45–63.
9. Sokolowski, M. B. & Hansell, K. P. (1992) *Genetica* **85,** 205–209.
10. Soll, D. R. (1995) *Int. Rev. Cytol.* **163,** 43–104.
11. Soll, D. R., Wessels, D., Voss, E. & Johnson, O. (2001) *Methods Mol. Biol.* **161,** 45–58.
12. Ghysen, A., Dambly-Chaudière, C., Aceves, E., Jan, L. Y. & Jan, Y. N. (1986) *Roux's Arch. Dev. Biol.* **195,** 281–289.
13. Bodmer, R. & Jan, Y. N. (1987) *Roux's Arch. Dev. Biol.* **196,** 69–77.
14. Siekhaus, D. E. & Fuller, R. S. (1999) *J. Neurosci.* **19,** 6942–6954.
15. Bate, M. (1999) *Curr. Opin. Neurobiol.* **9,** 670–675.
16. Nolo, R., Abbott, L. A. & Bellen, H. J. (2000) *Cell* **102,** 349–362.
17. Barclay, J. W., Atwood, H. L. & Robertson, R. M. (2002) *J. Comp. Physiol. A* **188,** 71–78.
18. Suster, M. L., Martin, J.-R., Sung, C. & Robinow, S. (2003) *J. Neurobiol.* **55,** 233–246.
19. Eberl, D. F., Duyk, G. M. & Perrimon, N. (1997) *Proc. Natl. Acad. Sci. USA* **94,** 14837–14842.
20. Kernan, M., Cowan, D. & Zuker, C. (1994) *Neuron* **12,** 1195–1206.
21. Jarman, A. P., Sun, Y., Jan, L. Y. & Jan, Y. N. (1995) *Development (Cambridge, U.K.)* **121,** 2019–2030.
22. Bloomquist, B. T., Shortridge, R. D., Schneuwly, S., Perdew, M., Montell, C., Steller, H., Rubin, G. M. & Pak, W. L. (1988) *Cell* **54,** 723–733.
23. Dettman, R. W., Turner, F. R., Hoyle, H. D. & Raff, E. C. (2001) *Genetics* **158,** 253–263.
24. Brewster, R. & Bodmer, R. (1995) *Development (Cambridge, U.K.)* **121,** 2923–2936.
25. Eberl, D. F., Hardy, R. W. & Kernan, M. (2000) *J. Neurosci.* **20,** 5981–5988.
26. Sawin-McCormack, E. P., Sokolowski, M. B. & Campos, A. R. (1995) *J. Neurogenet.* **10,** 119–135.
27. Daniel, A., Dumstrei, K., Lengyel, J. A. & Hartenstein, V. (1999) *Development (Cambridge, U.K.)* **126,** 2945–2954.
28. Suzuki, T. & Saigo, K. (2000) *Development (Cambridge, U.K.)* **127,** 1531–1540.
29. Liu, L., Yermolaieva, O., Johnson, W. A., Abboud, F. M. & Welsh, M. J. (2003) *Nat. Neurosci.* **6,** 267–273.
30. Tracey, W. D., Jr., Wilson, R. I., Laurent, G. & Benzer, S. (2003) *Cell* **113,** 261–273.
31. Walker, R. G., Willingham, A. T. & Zuker, C. S. (2000) *Science* **287,** 2229–2234.
32. Baker, J. D., Esenwa, V. & Kernan, M. (2001) *Mol. Biol. Cell* **12,** Suppl., 447a.
33. Han, Y.-G. & Kernan, M. J. (2001) *Mol. Biol. Cell* **12,** Suppl., 445a.
34. Chung, Y. D., Zhu, J., Han, Y.-G. & Kernan, M. J. (2001) *Neuron* **29,** 415–428.
35. Dubruille, R., Laurençon, A., Vandaele, C., Shishido, E., Coulon-Bublex, M., Swoboda, P., Couble, P., Kernan, M. & Durand, B. (2002) *Development (Cambridge, U.K.)* **129,** 5487–5498.
36. Kim, J., Chung, Y. D., Park, D.-y., Choi, S., Shin, D. W., Soh, H., Lee, H. W., Son, W., Yim, J., Park, C.-S., *et al.* (2003) *Nature* **424,** 81–84.
37. Jarman, A. P., Grau, Y., Jan, L. Y. & Jan, Y. N. (1993) *Cell* **73,** 1307–1321.
38. Caldwell, J. C. & Eberl, D. F. (2002) *J. Neurobiol.* **53,** 172–189.